

Geographical Centralization Resilience in Ethereum’s Block-Building Paradigms

SEN YANG*, Yale University, IC3, United States

BURAK ÖZ, Flashbots, Germany

FEI WU, King’s College London, United Kingdom

FAN ZHANG, Yale University, IC3, United States

Decentralization has an important geographic dimension that conventional metrics, such as stake distribution, often overlook. Where validators operate affects resilience to regional shocks (e.g., outages, natural disasters, or government intervention) as well as fairness in reward access. Yet in permissionless systems, validator locations cannot be prescribed by protocol rules; instead, they emerge endogenously from economic incentives. When certain locations offer systematic advantages, validators may strategically co-locate to maximize expected rewards, as observed in Ethereum, where validators cluster along the Atlantic corridor, which exhibits structurally favorable latency.

In this paper, we design and implement an agent-based simulation framework to study how Ethereum’s protocol design—particularly its block-building paradigms of local and external block building—interacts with validator and information-source distributions to shape geographical positioning incentives. Our simulations show that Ethereum’s block-building architecture is not geographically neutral: both paradigms induce location-dependent payoffs and migration incentives, with asymmetric access to information sources amplifying geographical centralization. We further demonstrate that consensus parameters, such as attestation thresholds and slot times, modulate latency sensitivity and can amplify these effects, acting as protocol-level levers. Finally, we discuss the implications of our findings for protocol design and outline potential mitigation directions informed by our analysis.

1 Introduction

Decentralization is the core security assumption of permissionless blockchains, underpinning key properties such as integrity, safety, availability, and censorship resistance [26, 40, 52, 59]. These properties typically rely on the assumption that at least a fraction of participants behave honestly, or that conflicting incentives prevent collusion—that is, that control and behavior are not highly centralized or correlated. Consequently, assessing decentralization requires more than identifying who controls mining power or stake; it must also account for the geographical distribution of participants.

Geographical decentralization is particularly important for two reasons. First, security assumptions depend on participants not being overly correlated. If a large share of validators are co-located, they become jointly vulnerable to external shocks like natural disasters or power outages, as well as jurisdictional risks such as government intervention. A prominent example is the 2021 ban on Bitcoin mining in China, which triggered a sharp and sudden drop in global hash rate and forced miners to relocate at scale [51]. Second, geography affects fairness: validators farther from network hubs may face persistent latency disadvantages that reduce their ability to compete for rewards.

Achieving geographical decentralization, however, is *non-trivial*. In permissionless blockchains, participant locations cannot be prescribed by protocol rules but instead emerge endogenously from their incentive structure. When certain locations offer systematic advantages, validators may strategically co-locate to maximize expected rewards, giving rise to location games reminiscent

*Work performed in part during an internship at Flashbots.

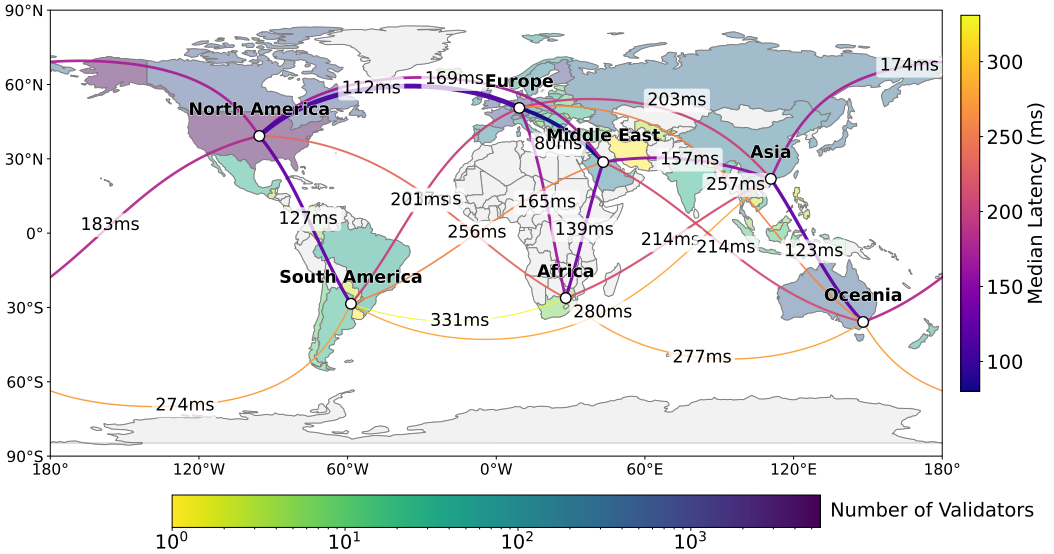


Fig. 1. Validator distribution and inter-region Internet latencies illustrate the geographic concentration of Ethereum validators and the latency landscape across regions. Validator location data covers ~16,000 Ethereum validators, provided by Chainbound [11]. Latency values are macro-regional medians of round-trip times between Google Cloud regions. Darker shading indicates a larger number of validators in a given country, showing that validators are primarily concentrated in the United States and Europe. Darker inter-regional links indicate lower average round-trip latency, highlighting the particularly low latency between North America and Europe relative to other regions.

of Hotelling’s law [31]. Ethereum provides a clear illustration: despite its large validator set, participation is heavily concentrated along the Atlantic corridor [11]—especially in the United States and Europe—where latency to other validators and infrastructure is most favorable (see Figure 1).

In this paper, we study how Ethereum’s protocol design, particularly its block-building architecture, systematically shapes the geographical positioning incentives of validators. Since a substantial fraction of validator rewards derives from block building [54], we focus on the two primary block-building paradigms currently used in Ethereum: *local block building*, where validators self-construct blocks and handle dissemination, and *external block building*, where validators outsource block construction and dissemination. We compare the migration incentives induced by these paradigms and evaluate their resilience to geographical centralization across different geographical distributions of information sources and validators, revealing paradigm-dependent and sometimes opposing centralization dynamics, as well as under varying consensus parameters such as attestation thresholds and slot duration.

We emphasize block-building paradigms and their interaction with consensus parameters because Ethereum is actively considering protocol changes that directly affect these dimensions, including an in-protocol block-outsourcing mechanism via enshrined Proposer-Builder Separation (ePBS) [24] and halving the slot duration [1]. Assessing the resulting geographical positioning incentives under these rules is critical for identifying protocol-level levers that may prevent validator concentration and the erosion of core security and fairness properties.

Empirical and theoretical limitations. While geographical decentralization has been studied through mining power or stake distributions [5, 13, 28] and empirical snapshots of validator locations [10, 22, 33], these approaches remain limited. They describe the current distribution

but cannot predict counterfactual outcomes or the effects of future protocol changes. Moreover, empirical measurements conflate multiple influences—including infrastructure, protocol-level mechanisms, and heterogeneous validator strategies—making causal attribution difficult. Purely theoretical analyses face complementary limitations: the interaction of heterogeneous strategies, network latencies, and protocol rules induces a state space that is too complex for tractable modeling.

Addressing the gaps with simulation. To overcome the limitations of empirical and theoretical approaches, and to accommodate heterogeneous agent behavior and interactions with protocol components under heterogeneous geographic and latency conditions, we develop an agent-based simulation framework [38]. Unlike empirical measurements, our framework enables counterfactual analysis and controlled variation of key factors, allowing us to isolate the effects of block-building paradigms on migration incentives and resulting validator geography. This approach provides a systematic view of how geographic concentration impacts Ethereum’s decentralization and liveness.

To the best of our knowledge, this is the first work to provide a simulation-based analysis of how Ethereum’s block-building mechanisms, validator and information-source distributions, and consensus parameters jointly shape validators’ geographical positioning incentives and the emergence and persistence of spatial concentration.

We make the following contributions:

- We design and implement an agent-based simulation framework that models validator behavior under Ethereum’s consensus protocol, enabling controlled experimentation across geographic, infrastructural, and protocol configurations.
- Using a model calibrated with real-world latency data, we analyze how Ethereum’s two block-building paradigms—local block building and external block building—interact with validator and information-source distributions to shape validators’ geographical positioning incentives.
- We show that Ethereum’s block-building architecture is not geographically neutral: both paradigms induce location-dependent payoffs and migration incentives, with asymmetric access to information sources amplifying geographical centralization. We further demonstrate that consensus parameters, such as attestation thresholds and slot times, modulate latency sensitivity and can amplify these effects.
- We discuss the implications of our findings for protocol design and outline potential mitigation directions informed by our analysis.
- We release the simulation framework and a public dashboard of our results [3, 4] to support reproducibility and future research on geographical decentralization.

2 Background

Proof-of-Stake Ethereum. Ethereum has operated under Proof-of-Stake (PoS) since September 2022 [21]. In PoS, any participant can become a validator by depositing at least 32 ETH as collateral, which aligns incentives with the network’s security [9]. Block production under PoS follows the proposer–attester model. In each 12-second slot, a validator is pseudorandomly selected as the *proposer* to create and broadcast a new block. A committee of validators, also pseudorandomly selected from the active validator set, serves as *attesters* by making attestations on the proposed block. The block is considered valid only if it receives the required number of attestations, as mandated by the protocol.

Maximal Extractable Value. Maximal Extractable Value (MEV) refers to the value that privileged entities (e.g., proposers) can capture by inserting, excluding, or reordering transactions within a block [14]. MEV poses a threat to decentralization by skewing the reward distribution, which in principle should be homogeneous across validators given equal stake. Since effective extraction

requires substantial capital, specialized infrastructure, and sophisticated algorithms, MEV can foster centralization by concentrating rewards among well-resourced actors [19].

Proposer-Builder Separation. Proposer-Builder Separation (PBS) is introduced to enable validators to outsource block building (and MEV extraction) to specialized entities called *builders*, allowing them to benefit from MEV rewards regardless of their resources or infrastructure, while reducing centralization pressure. PBS is currently implemented out of the Ethereum protocol via MEV-Boost [23], where the proposer conducts an auction among builders through a trusted third party (*relay*) to obtain the most valuable block. PBS will be integrated at the protocol level (referred to as ePBS) in Ethereum’s upcoming “Glamsterdam” upgrade, where relay dependencies are removed, and proposers can access bids from builders directly [24]. Under PBS, the MEV of a transaction typically refers to the priority fee plus direct transfer to the builder from order flow providers (e.g., searchers) alongside their transaction [44, 55]. A proposer may strategically delay block publishing to gain additional MEV from transactions arriving later. This behavior is known as timing games [43, 46].

Agent-Based Modeling. Agent-Based Modeling (ABM) studies complex systems by specifying individual entities (*agents*) and the rules governing their behaviors [38]. It is particularly suited to settings with heterogeneous participants, adaptive decision-making, and interactions that resist closed-form analysis. An ABM typically consists of agents situated in an *environment*, each following a set of *strategies*. The environment provides context and constraints, while agents respond based on their strategies. By modeling and simulating local interactions, ABM reveals how individual incentives generate emergent system-level outcomes.

3 Simulation Framework

In this section, we present our agent-based simulation framework. We first introduce a base model that captures geographical and latency assumptions, agent characteristics, environmental components such as the consensus protocol and information sources, and the agents’ strategy space. We then describe the two block-building paradigms we study, which differ in how validators capture rewards and fulfill consensus duties. Finally, we define the metrics used to quantify geographical centralization under these paradigms. The symbols used throughout the model are summarized in Table 2.

3.1 Base Model

Our model builds on ABM techniques and captures the heterogeneous validator strategies and their interactions under the consensus protocol. The system consists of autonomous agents whose incentive-driven behaviors collectively generate global outcomes. The canonical components of the model are as follows.

Geographical regions and latency. We model geography as a finite set of discrete regions $\mathcal{R} = \{r_1, r_2, \dots, r_m\}$. For any two regions $r_j, r_k \in \mathcal{R}$, define the random propagation latency of a message $d(r_j, r_k)$. We assume $d(r_j, r_k)$ is drawn from a log-normal distribution with parameters known to agents $\ln[d(r_j, r_k)] \sim \mathcal{N}(\mu_{jk}, \sigma^2)$, and the expected latency can be given by $\mathbb{E}[d(r_j, r_k)] = e^{\mu_{jk} + \sigma^2/2}$. This abstraction simplifies geographical modeling and reflects empirical network behavior, as inter-region latencies are influenced by routing and infrastructure and do not necessarily increase with geographical distance. The log-normal distribution allows us to capture the heavy-tailed nature of network latency, where rare but high-latency events can affect block propagation and attestation.

Agents. Each validator in the set $\mathcal{V} = \{v_1, \dots, v_p\}$ is modeled as an autonomous agent. An agent v_i is characterized by the following attributes:

- *Stake* $s_i \in \mathbb{R}_{\geq 0}$, which determines both the probability of proposer selection and attestation weight. For tractability, we assume that all validators hold equal and constant stakes.
- *Region* $r_i \in \mathcal{R}$, which determines the latency for messages exchanged with other agents.

Environment. The environment consists of two components: (i) the consensus protocol, which governs time, proposer selection, and attestation; and (ii) information sources, which determine the value of blocks proposed by the validators. We describe each in turn.

Time and consensus. Drawing from the timing games model in [46], we partition time into slots $n \in \{1, \dots, N\}$ of fixed duration $\Delta > 0$. In each slot n , a validator is selected as the proposer p_n , and a set of attesters $\mathcal{A}_n \subseteq \mathcal{V} \setminus \{p_n\}$ is assigned to vote on the proposal. A block becomes canonical if at least a fraction $\gamma \in (0, 1]$ of attesters in \mathcal{A}_n vote positively before a cutoff time $\tau_{\text{cut}} \in [0, \Delta]$. The timeliness of attester votes depends on both the block’s release time and the propagation latencies. We abstract away the details of fork-choice rules.

Information Sources: Signal and Supplier. We define an information source $I \in \mathcal{I}$ as an exogenous generator of block value for the proposer. Each source is associated with a geographic region $r(I) \in \mathcal{R}$, which determines its latency to the proposer and, consequently, the freshness of the information it provides. We assume information sources to be fungible, with identical value-generation parameters. To isolate the effects of geography, we vary only their spatial distribution, enabling a controlled comparison between homogeneous and heterogeneous placements and their impact on validator incentives.

We distinguish two types of information sources: $\mathcal{I}_{\text{signal}} \subseteq \mathcal{I}$ and $\mathcal{I}_{\text{supplier}} \subseteq \mathcal{I}$. A *signal* source contributes only partially to the block value—for example, a centralized exchange providing price information that can be arbitrated on-chain. Proposers aggregate value from multiple such signal sources when constructing a block. A *supplier*, by contrast, fully determines the value of the proposed block, as in PBS, where an external party delivers a complete block. In this case, the proposer captures value from a single supplier source.

Formally, let $V_I(t)$ denote the value available from source I at elapsed time t within a slot, capturing the temporal evolution of extractable value [43, 46, 53]. For tractability, we model $V_I(t)$ as a deterministic linear function $V_I(t) = a_I t + b_I$, where $a_I > 0$ denotes the growth rate of extractable value¹ and $b_I > 0$ is the initial value at the start of the slot, representing transactions accumulated since the previous block.²

Strategy Space. We focus on two strategic choices available to a proposer in a slot:

- *Timing:* The proposer chooses a block release time $\tau \in [0, \tau_{\text{cut}}]$, which affects both attestation success and utility.
- *Migration:* Proposers may migrate between regions at a cost c . We model migration as instantaneous, justified by pre-synchronization of validator nodes across multiple regions.

3.2 Block-Building Paradigms

Block building is a critical duty for Ethereum validators and a major source of their rewards. An honest but economically rational validator seeks to optimize along two dimensions: (i) constructing a high-value block by capturing MEV from transactions, and (ii) ensuring that the block becomes canonical by proposing a valid block on time and reaching a sufficient number of attesters. These

¹In practice, order flow may evolve non-linearly. For example, arbitrage opportunities may surge shortly before block proposal in response to external price movements.

²The initial value b_I corresponds to the reward a proposer would obtain by releasing the block immediately, i.e., without delaying to exploit timing games.

objectives are inherently in tension due to timing-game incentives, whereby validators may delay block proposal to increase block value at the risk of missing consensus deadlines [43, 46].

We focus on the two primary block-building paradigms adopted by Ethereum validators:

- **Local Block Building:** The validator collects signals—such as price information and transactions—from a distributed set of information sources (e.g., centralized exchange servers, wallet RPC endpoints) and locally constructs the block. It then signs the block header and propagates the block to the network, aiming to reach sufficient attesters before the consensus deadline.
- **External Block Building:** The validator outsources block construction to a third-party supplier, such as a builder in the PBS design. The validator blindly signs the provided block header, returns it to the supplier, and relies on the supplier to propagate the block to the network, again aiming to reach sufficient attesters on time.

Figure 2 illustrates the operational dynamics of the two block-building paradigms.

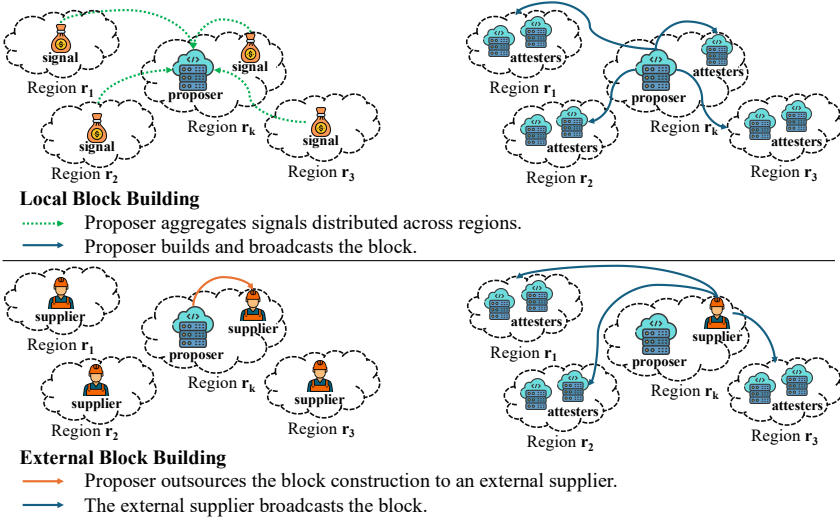


Fig. 2. Block production and dissemination under the Local and External block-building paradigms.

3.2.1 Model: Local Block Building. In the local block-building model, a proposer’s payoff depends on two latency components: (i) latencies to information sources, which determine how much block value can be incorporated at proposal time, and (ii) latencies to attesters, which determine whether the proposed block is voted canonical after release.

If a proposer p_n located in region $r(p_n)$ releases a block at time τ , it incorporates value from each signal source $I \in \mathcal{I}_{\text{signal}}$ as observed at an earlier time $\tau - d(r(p_n), r(I))$, accounting for network latency. The value contributed by source I is therefore

$$V_I(\tau - d(r(p_n), r(I))).$$

We assume that values from different signal sources are additive, i.e., sources do not generate overlapping transactions. Generalizing to an arbitrary proposer located in region $r \in \mathcal{R}$, the aggregate block value available at release time τ is given by

$$V_r(\tau) = \sum_{I \in \mathcal{I}_{\text{signal}}} V_I(\tau - d(r, r(I))).$$

Attestation success. Upon release, each attester $a \in \mathcal{A}_n$ located in region $r(a)$ receives the block after a latency $d(r, r(a))$, drawn from a log-normal with Cumulative Distribution Function (CDF) $F_{d(r, r(a))}$. An attester a votes on time if $\tau + d(r, r(a)) \leq \tau_{\text{cut}}$, which occurs with probability

$$q_a(\tau; r) = F_{d(r, r(a))}(\tau_{\text{cut}} - \tau) \mathbf{1}\{\tau < \tau_{\text{cut}}\}.$$

Let

$$S(\tau; r) = \sum_{a \in \mathcal{A}_n} \text{Bernoulli}(q_a(\tau; r))$$

denote the number of timely attestations. Then $S(\tau; r)$ follows a Poisson–binomial distribution, and the probability that the block becomes canonical is

$$\Pi_r(\tau) = \Pr\left[S(\tau; r) \geq \lceil \gamma |\mathcal{A}_n| \rceil\right].$$

Optimal release time. A proposer located in region r aims to release its block as late as possible to maximize $V_r(\tau)$, subject to maintaining a sufficiently high probability of canonicalization. Since $V_r(\tau)$ is modeled as deterministic and the latency distributions are known, the proposer solves, at the start of each slot, the following optimization problem:

$$\tau_r^* = \max\{\tau \in [0, \tau_{\text{cut}}] : \Pi_r(\tau) \geq R\},$$

where R represents the proposer's risk tolerance, capturing its willingness to engage in timing games at the cost of a higher probability that the block fails to reach some attesters. The corresponding expected payoff is

$$W(r) = \Pi_r(\tau_r^*) V_r(\tau_r^*).$$

REMARK. For a large committee $|\mathcal{A}_n|$, the randomness of $S(\tau; r)$ concentrates around its mean. By the Law of Large Numbers, defining

$$\zeta_r(\tau) = \frac{1}{|\mathcal{A}_n|} \sum_{a \in \mathcal{A}_n} q_a(\tau; r),$$

we obtain the approximation $\Pi_r(\tau) \approx \mathbf{1}\{\zeta_r(\tau) \geq \gamma\}$. Under this approximation, τ_r^* corresponds to the critical release time at which $\zeta_r(\tau)$ falls below the attestation threshold γ .

Migration decision. At the start of each slot, the proposer compares its expected payoff $W(r)$ across all regions $r \in \mathcal{R}$. Since migration incurs a cost c , the proposer relocates from its current region $r(p_n)$ only if the marginal benefit of migration exceeds this cost:

$$\max_{r \in \mathcal{R} \setminus \{r(p_n)\}} W(r) - W(r(p_n)) > c.$$

In this case, the proposer relocates to

$$r^* = \arg \max_{r \in \mathcal{R} \setminus \{r(p_n)\}} W(r),$$

and releases the block at the corresponding optimal time $\tau_{r^*}^*$. Otherwise, it remains in $r(p_n)$ and releases at $\tau_{r(p_n)}^*$.

This formulation captures proposers' strategic behavior in jointly optimizing release timing and geographical location to maximize expected payoff.

Model justification. Under local block-building, we model proposers as aggregating signals from geographically distributed information sources, with total block value evolving over time. This captures self-building proposer behavior, in which blocks are continuously updated as new order flow arrives. We explicitly account for proposers' latency to attesters to determine how long they can engage in timing games by delaying block release while still satisfying consensus deadlines.

3.2.2 Model: External Block Building. In the external block-building model, two aspects differ from the local block-building case: (i) block value is supplied directly by a block supplier rather than aggregated from multiple signal sources, and (ii) block propagation originates from the selected supplier's region rather than the proposer's. Consequently, the proposer's payoff depends on both its latency to the supplier and the supplier's latency to attesters.

If a proposer p_n located in region $r(p_n)$ considers a block supplier $I \in \mathcal{I}_{\text{supplier}}$ located in region $r(I)$, it observes the supplier's offered value with latency $d(r(p_n), r(I))$. At release time τ , the effective value provided by supplier I is therefore

$$V_I(\tau) = V_I(\tau - d(r(p_n), r(I))).$$

Attestation success. Once selected by the proposer, a supplier I located in region $r(I)$ broadcasts the block to attesters. Relative to the local block-building model, an additional latency $d(r(p_n), r(I))$ is incurred between the proposer and the supplier. As a result, the timely-attestation probability becomes supplier-specific:

$$q_a(\tau; I) = F_{d(r(p_n), r(I)) + d(r(I), r(a))}(\tau_{\text{cut}} - \tau) \mathbf{1}\{\tau < \tau_{\text{cut}}\}.$$

The probability that the block becomes canonical is therefore

$$\Pi_I(\tau) = \Pr\left[S(\tau; I) \geq \lceil \gamma |\mathcal{A}_n| \rceil\right],$$

where $S(\tau; I)$ is defined analogously to the local block-building case.

Optimal release time. For each supplier I , conditional on selecting I , the proposer chooses a release time

$$\tau_I^* = \max\{\tau \in [0, \tau_{\text{cut}}] : \Pi_I(\tau) \geq R\},$$

and obtains the expected payoff

$$W(I) = \Pi_I(\tau_I^*) V_I(\tau_I^*).$$

Migration decision. At the start of each slot, the proposer compares the expected payoff obtained by selecting the best available supplier overall—potentially requiring migration—to that obtained from the best supplier accessible without changing location. Let

$$W^{\text{stay}} = \max_{I \in \mathcal{I}_{\text{supplier}}(r(p_n))} W(I)$$

denote the maximum expected payoff achievable without migrating. The proposer migrates if and only if

$$\max_{I \in \mathcal{I}_{\text{supplier}}} W(I) - W^{\text{stay}} > c.$$

In this case, it relocates to the region of a supplier

$$I^* \in \arg \max_{I \in \mathcal{I}_{\text{supplier}}} W(I),$$

and releases the block at the corresponding optimal time $\tau_{I^*}^*$. Otherwise, the proposer remains in $r(p_n)$ and selects the best locally accessible supplier.

Model justification. Under external block-building, we intentionally abstract away the signal-aggregation process and model each block supplier as delivering a fully constructed block whose value evolves over time. This reflects proposer behavior under PBS, where proposers neither observe nor control underlying order-flow sources or builder competition, but instead choose when to select and release a supplied block.

While, in practice, block suppliers aggregate geographically distributed order flow, these interactions primarily affect the level of block value rather than the propagation dynamics that

determine attestation success and canonicalization. Our model therefore isolates the geographical incentives induced by block origination and dissemination—the latter being the focus of this work. Moreover, increasing vertical integration among order-flow providers, builders, and relays further supports modeling suppliers as unified block-providing endpoints from the proposer’s perspective [15, 44, 55, 59].

3.3 Evaluation Metrics

We next introduce metrics that quantify geographical centralization in our simulations. To characterize how stake is distributed across geographical units (countries/regions; hereafter “regions”), we use the Gini coefficient (inequality, denoted Gini_g) and the Herfindahl–Hirschman Index (concentration, denoted HHI_g). To capture variation in proposer incentives across regions, we define the geographical payoff coefficient of variation, CV_g , which measures disparities in the best proposer payoffs across regions within a slot. Finally, to quantify how geography impacts consensus liveness, we define the geographical liveness coefficient, LC_g , which reflects the minimum number of regions whose failure can break Ethereum’s liveness. Together, these metrics capture stake inequality and concentration, incentive disparities, and resilience to correlated regional failures.

Formally, let \mathcal{R} denote the set of regions. For each $r \in \mathcal{R}$, let s_r be the total effective balance of validators located in r , and let $S = \sum_{r \in \mathcal{R}} s_r$. Define normalized shares

$$w_r = \frac{s_r}{S}, \quad w_r \geq 0, \quad \sum_{r \in \mathcal{R}} w_r = 1.$$

Geographical Gini. The geographical Gini coefficient is

$$\text{Gini}_g = \frac{1}{2|\mathcal{R}|} \sum_{r \in \mathcal{R}} \sum_{r' \in \mathcal{R}} |w_r - w_{r'}|.$$

It equals 0 under perfectly even stake distribution and increases with inequality (approaching $1 - 1/|\mathcal{R}|$ in the extreme of all stakes in one region).

Geographical HHI. The geographical HHI is

$$\text{HHI}_g = \sum_{r \in \mathcal{R}} w_r^2,$$

with $\text{HHI}_g \in [1/|\mathcal{R}|, 1]$. Lower values indicate greater dispersion.

Geographical Payoff Coefficient of Variation (CV). Let \mathcal{W} denote the set of best payoffs for the proposer in region $r \in \mathcal{R}$ in one slot, the geographical payoff coefficient of variation is

$$\text{CV}_g = \frac{\sigma(\mathcal{W})}{\mu(\mathcal{W})},$$

where $\mu(\mathcal{W})$ and $\sigma(\mathcal{W})$ are the mean and standard deviation of \mathcal{W} , respectively. It grows as inter-regional disparities increase.

Liveness coefficient. To capture robustness against geographically correlated failures (e.g., natural disasters or country-level regulation), we adapt the Nakamoto coefficient to Ethereum PoS liveness. Ethereum PoS maintains liveness as long as at least $2/3$ of the effective stake is online. Sort regions by stake share w_r in non-increasing order and let r_1, r_2, \dots denote that ordering. The *liveness coefficient* (LC_g) is the minimal k such that

$$\sum_{i=1}^k w_{r_i} \geq \frac{1}{3}.$$

Intuitively, it is the smallest number of (largest) regions whose simultaneous outage suffices to threaten liveness. Larger values indicate greater resilience.

4 Simulation Experiments

In this section, we use our simulation framework to study how Ethereum block-building paradigms interact with validator and information-source distributions, as well as consensus parameters, to shape validators’ migration incentives and the resulting degree of geographical centralization. Unless stated otherwise, we use a baseline configuration in which both validators and information sources are uniformly distributed across regions. We design four classes of Simulation Experiments (SEs) to isolate the impact of block-building paradigms along key dimensions of interest:

- **SE 1 (Information-Source Placement Effect):** Assuming a uniformly distributed validator set and holding network, economic, and consensus parameters fixed, we examine how the geographical placement of information sources affects validators’ migration incentives under local and external block-building paradigms.
- **SE 2 (Validator Distribution Effect):** Assuming a uniformly distributed set of information sources and holding network, economic, and consensus parameters fixed, we examine how the initial geographical distribution of validators affects migration incentives under local and external block-building paradigms.
- **SE 3 (Joint Heterogeneity):** Assuming heterogeneous geographical distributions of both validators and information sources and holding network, economic, and consensus parameters fixed, we examine how joint spatial heterogeneity shapes validators’ migration incentives under local and external block-building paradigms.
- **SE 4 (Consensus-Parameter Effect):** Assuming uniformly distributed validators and information sources and holding network and economic parameters fixed, we examine how variations in consensus parameters affect validators’ migration incentives under local and external block-building paradigms.

4.1 Simulation Setup

We next specify the setup of our simulation framework.

- **Discrete time:** Time is modeled in discrete steps, with each step corresponding to 50ms to approximate the continuous flow of real time.
- **Simultaneity:** The validators act simultaneously at each time step. For example, once the proposer releases a block, attestors in the same region can immediately attest to it.
- **Regions:** We calibrated the set of regions \mathcal{R} using data from Google Cloud Platform (GCP), which covers 40 regions worldwide. These GCP regions can be further aggregated into seven macro-regions, as detailed in [Appendix A](#).
- **Latency:** We calibrated the log-normal distribution μ such that expected latency equals the empirical mean latency measured between the corresponding regions on Google Cloud [27]. These measurements are based on two-way delays reported by Google Cloud’s public inter-region latency data, ensuring that our simulation reflects realistic wide-area network conditions. We set $\sigma = 0.5$, but the result can be analogous for other values.
- **Consensus:** We follow the standard Ethereum consensus parameters [20] by setting $\Delta = 12s$, $\tau_{\text{cut}} = 4s$, and $\gamma = 2/3$, and assume that all proposers aim to ensure their block becomes canonical with $R = 99\%$. Finally, in all cases, we set $|\mathcal{V}| = 1,000$ validators and $N = 10,000$ slots.³

³As shown in [Appendix D](#), this configuration preserves similar qualitative trends observed at larger scales while providing a practical balance between computational feasibility and statistical stability.

- **Information sources:** For signal sources, we set the value parameters $(a_I, b_I) = (0.01, 0.001)$, and suppliers are parameterized such that their value matches the *aggregate* signal value available to a proposer in the baseline configuration, with $(a_I, b_I) = (0.4, 0.04)$. That is, a supplier’s offered value is scaled to be comparable to the total value that would be obtained by aggregating all signal sources under local block building.

Since our analysis focuses on how information-source placement and propagation latency shape validators’ migration incentives, the absolute scale of block value is not central, provided values are matched across paradigms. We therefore adopt fixed reference parameters rather than time-varying values, abstracting away from the value progress and bidding dynamics observed in today’s MEV-Boost auctions.

- **Migration cost:** We first run a baseline simulation with $c = 0$ and, for each of the first 1,000 slots,⁴ record the marginal benefit of migrating to the proposer’s best alternative region. The resulting distributions of marginal benefits under both block-building paradigms are shown in [Figure 10](#). Following the Pareto principle, we set $c = 0.002$, which prevents approximately 80% of migration events in the baseline simulation under the external block-building paradigm. We present results for alternative migration-cost settings in [Appendix E](#).

Implementation. We implement our simulation framework using Mesa, a Python-based ABM framework [50]. The framework consists of about 2.5K lines of code. We conducted experiments on a testbed equipped with an Intel Xeon Platinum 8380 CPU (80 cores), and 128 GB of RAM, running 64-bit Ubuntu 22.04 as the operating system.

4.2 Baseline Configuration and Outcomes

We first report outcomes under the baseline configuration, in which both validators and information sources are uniformly distributed across macro-regions and evenly within each macro-region’s GCP regions. This avoids bias arising from the uneven global distribution of GCP regions,⁵ ensuring parity in both validator density and aggregate information value across macro-regions.

While MEV-Boost relays (similar to suppliers in our framework) are unevenly distributed across regions today, this asymmetry largely reflects architectural features of the current relay-based design. Under ePBS, block production and propagation are expected to be carried out by builders directly, who may be more geographically distributed [16]. We therefore use this configuration as a neutral baseline for isolating how protocol design alone shapes validator incentives over a fixed Internet infrastructure. Unless stated otherwise, all subsequent results are interpreted relative to this baseline.

[Figure 3](#) shows the evolution of our metrics under the baseline configuration across simulated slots. Under both paradigms, the $Gini_g$ and HHI_g indices increase over time while the liveness coefficient (LC_g) declines, indicating growing *centralization* even from an initially uniform distribution. However, the rate and degree of convergence differ markedly: migration incentives are amplified under the local block-building paradigm, as reflected in faster concentration dynamics and a higher reward-variance coefficient (CV_g).

These differences arise from how migration affects payoffs under each paradigm. Under local block building, proposers are jointly sensitive to the location of signal sources—for value accrual—and to the location of other validators—for timely block dissemination. By contrast, when block construction and dissemination are outsourced, block propagation is decoupled from proposer location; the marginal benefit of migration is driven primarily by latency to the selected supplier,

⁴We focus on the first 1,000 slots to capture pre-steady-state incentives: with $c = 0$ validators quickly relocate toward high-payoff regions, after which marginal benefit collapse toward zero. Using an early window avoids this collapse.

⁵GCP regions are heavily concentrated in Europe, North America, and Asia (see [Appendix A](#)).

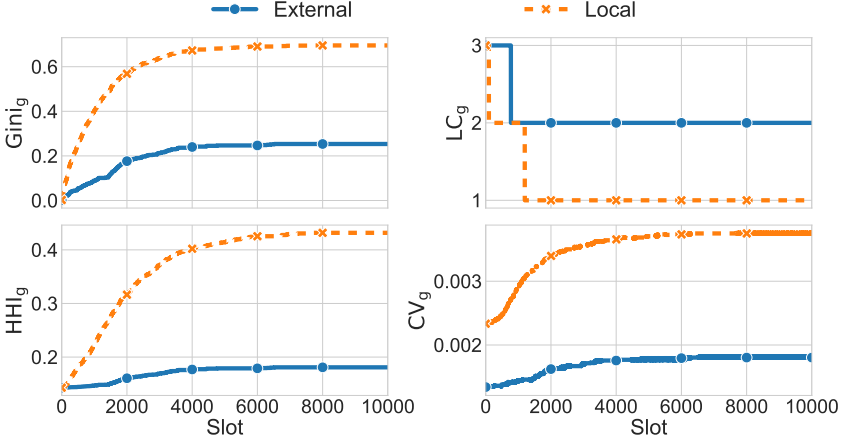


Fig. 3. *Baseline configuration (homogeneous validators and information sources)*. Evolution of centralization metrics under Local and External block-building paradigms.

which is comparatively less decisive. As a result, migration incentives—and ultimately geographical centralization—are weaker under external block building in the baseline configuration.

In [Appendix F](#), we present a detailed analysis of the validators’ convergence locus.

4.3 SE 1: Information-Source Placement Effect

Holding validator placement fixed at the baseline configuration, we vary the geographical placement of information sources to examine how validators’ migration incentives differ under local and external block-building paradigms. Specifically, we consider two contrasting information-source placements that differ in their average network latency to validators. This design isolates how protocol design interacts with information-source geography to shape migration incentives.

We consider the following two configurations:

- *Latency-aligned*: Three information sources are placed in low-latency regions—asia-northeast1, europe-west1, and us-east4—yielding low average latency to validators.
- *Latency-misaligned*: Three information sources are placed in high-latency regions—afrika-south1, australia-southeast1, and southamerica-east1—resulting in significantly higher average latency.

Across both configurations, supplier value parameters and signal-source calibration are kept identical to the baseline, ensuring that observed differences arise solely from geographical placement rather than changes in aggregate information value.

[Figure 4](#) shows the evolution of our metrics under latency-aligned and latency-misaligned information-source placements, together with the baseline configuration as a reference. Under both block-building paradigms, asymmetric information-source placement leads to faster and stronger geographical centralization, a sharper decline in the liveness coefficient, and higher reward variance

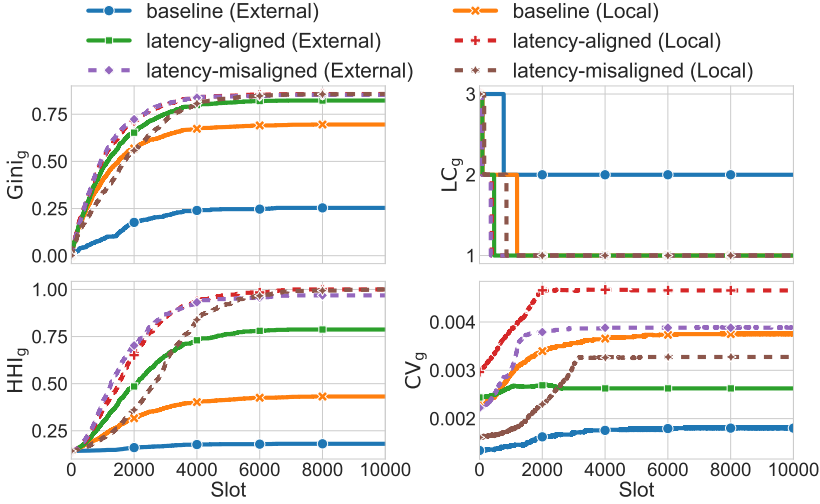


Fig. 4. *Information-source placement effect (homogeneous validators)*. Evolution of centralization metrics under Local and External block-building paradigms for latency-aligned and latency-misaligned information-source placements.

across regions.⁶ This is consistent with the intuition that asymmetries in access to rewards amplify validators’ incentives to migrate.

However, the two paradigms exhibit opposite sensitivities to the specific placement of information sources. Under local block building, the latency-aligned configuration centralizes more rapidly, with lower liveness and higher reward variance than the latency-misaligned case. In contrast, under external block building, the latency-misaligned configuration exhibits stronger centralization dynamics.

The stronger centralization observed under asymmetric information-source placement arises from how migration interacts with source geography under each block-building paradigm.

Under local block building, locating in a low-latency region simultaneously improves access to signal sources and propagation to attesters, increasing the marginal benefit of migration and making it more likely to exceed the migration cost. Under external block building, by contrast, when suppliers are located in poorly connected regions, non-colocated proposers face large proposer–supplier latencies; migrating closer to the supplier therefore yields a larger payoff increase, more frequently justifying relocation. In this paradigm, the proposer can influence only its latency to the supplier, while proximity to other validators provides no direct benefit, as block dissemination is handled by the supplier.

Overall, these results show that unbalanced information-source placement amplifies migration incentives relative to the balanced baseline. The extent and direction of this amplification depend critically on the adopted block-building paradigm, with different placements either accelerating or dampening geographical centralization.

⁶An exception arises under the local block-building paradigm in the latency-misaligned configuration, which both starts and converges to a lower reward-variance coefficient than the baseline. This behavior likely reflects a trade-off between high-latency regions hosting the information sources, which offer higher marginal value growth over time but suffer from slower propagation to attesters, and low-latency regions, which exhibit the opposite characteristics. The resulting tension leads to a more balanced distribution of rewards across regions relative to the baseline.

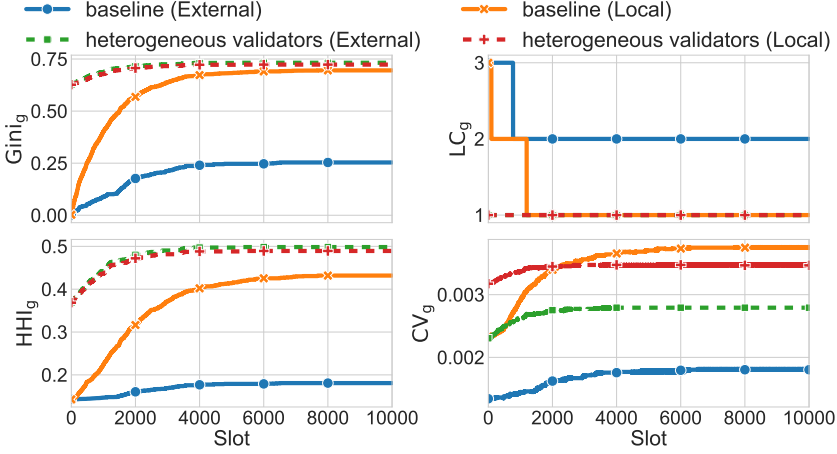


Fig. 5. *Validator distribution effect (homogeneous information sources)*. Evolution of centralization metrics under Local and External block-building paradigms with a heterogeneous validator distribution.

4.4 SE 2: Validator Distribution Effect

Holding information-source placement fixed at the baseline configuration, we vary the initial geographical distribution of validators to examine how migration incentives differ under local and external block-building paradigms. Specifically, we initialize validators according to Ethereum’s current geographic distribution [11], which exhibits substantial concentration in the United States and Europe (see Figure 1). This design isolates how protocol design interacts with validator geography to shape migration incentives.

Figure 5 shows the evolution of our metrics under a heterogeneous validator distribution, together with the baseline configuration as a reference. Because the initial validator distribution is already geographically concentrated, centralization metrics are elevated and the liveness coefficient is lower at the outset compared to the baseline, which starts from a neutral configuration. Reward variance is likewise higher initially, reflecting pre-existing regional disparities in validator density.

Under both block-building paradigms, this initial concentration leads to rapid convergence toward an equilibrium in which most validators become co-located. Once this state is reached, the marginal benefits of further migration no longer exceed the migration cost. Unlike in the baseline case, the two paradigms exhibit no substantial differences in either the speed or degree of convergence: when incumbent hubs already exist, migration benefits quickly saturate under both paradigms, whereas in the baseline configuration, such hubs emerge endogenously over time and primarily under local block building.

Consistent with earlier results, reward variance remains higher under local block building. However, relative to its baseline, external block building exhibits a stronger amplification of inter-regional reward disparities when validators are already clustered, as propagation advantages translate more directly into payoff asymmetries. By contrast, under local block building, rapid convergence to a dominant hub limits further differentiation, causing reward variance to stabilize once migration saturates.

Overall, these results indicate that when validator geography is already centralized, the currently active block-building paradigms in Ethereum induce similar migration dynamics, with rapid convergence toward co-location and limited scope for further relocation.

4.5 SE 3: Joint Heterogeneity

We jointly vary the geographical placement of information sources and the initial distribution of validators to examine how migration incentives differ under local and external block-building paradigms when both dimensions are heterogeneous. Specifically, we combine the latency-aligned and latency-misaligned information-source placements from [Section 4.3](#) with the empirically observed validator distribution from [Section 4.4](#). Results are compared against the baseline configuration in which both validators and information sources are uniformly distributed.

This experiment captures interaction effects between validator geography and information-source placement, illustrating how joint spatial heterogeneity shapes migration incentives beyond the effects observed when each dimension is varied in isolation.

[Figure 6](#) shows the evolution of our metrics under latency-aligned and latency-misaligned information-source placements with a heterogeneous validator distribution, together with the baseline configuration as a reference. Overall, the results closely mirror those in [Section 4.3](#) and [Section 4.4](#): as in [Section 4.3](#), asymmetric information-source placement leads to stronger geographical centralization, and as in [Section 4.4](#), starting from an already concentrated validator distribution results in rapid convergence toward an equilibrium in which the marginal benefits of further migration no longer exceed the migration cost.

The primary deviation arises under the external block-building paradigm when information sources are placed in high-latency regions. As in [Section 4.3](#), co-locating with suppliers in poorly connected regions yields a large payoff gain, since proposer–supplier latency is the only delay the proposer can directly influence in this paradigm. In the joint heterogeneity setting, validators are initially concentrated in low-latency regions, reflecting today’s Ethereum geography. This produces a transient phase in which some validators migrate away from incumbent hubs, briefly improving geographical decentralization. Over time, because block propagation is handled by the supplier and proximity to other validators provides no direct benefit, incentives to co-locate with suppliers dominate, leading to convergence toward a single supplier region and renewed geographical centralization. In [Appendix G](#), we present a detailed analysis of validators’ convergence locus under this joint heterogeneity setting.

Overall, these results indicate that under joint spatial heterogeneity of validators and information sources, the system starts from a highly centralized state and rapidly converges to a saturated equilibrium in which further migration yields little benefit. While the strength of these effects depends on the adopted block-building paradigm and the placement of information sources, both settings ultimately exhibit stronger geographical centralization than the baseline configuration, weakening decentralization guarantees.

4.6 SE 4: Consensus-Parameter Effect

Holding validator and information-source placements fixed at the baseline configuration, we vary consensus parameters to examine how validators’ migration incentives differ under local and external block-building paradigms. Specifically, we consider (i) different attestation threshold values and (ii) different slot times.

4.6.1 Attestation Threshold Effect. We analyze how changing the required attestation threshold γ —the quorum needed for a block to become canonical—affects migration incentives. We consider $\gamma \in \{\frac{1}{3}, \frac{1}{2}, \frac{2}{3}, \frac{4}{5}\}$, reflecting alternative design choices that trade off safety, liveness, and economic penalties, and have been actively discussed in recent consensus design work [8].

[Figure 7](#) shows the evolution of our metrics under different attestation thresholds, including the baseline value. Across all thresholds, centralization pressure is consistently stronger under local block building, reflected in higher Gini and HHI indices, lower liveness coefficients, and greater

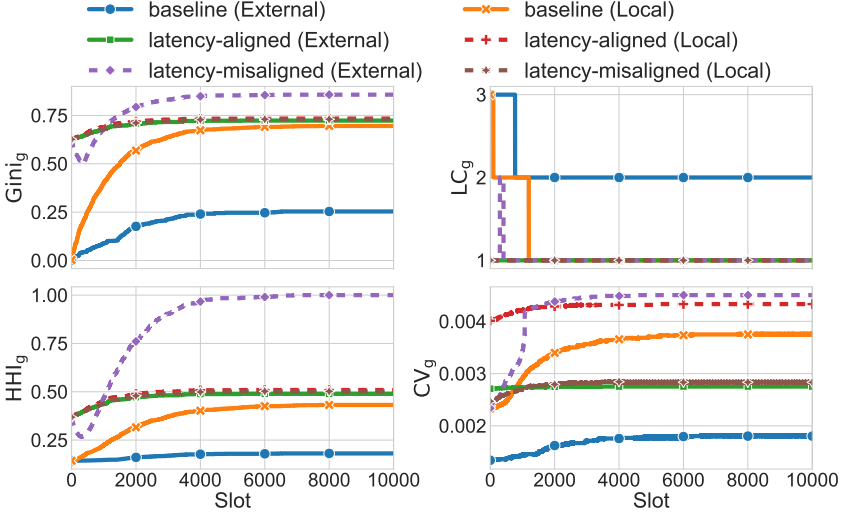


Fig. 6. Joint heterogeneity (validators and information sources). Evolution of centralization metrics under Local and External block-building paradigms for latency-aligned and latency-misaligned information-source placements with heterogeneous validator distribution.

reward disparity. However, the impact of varying γ differs markedly between the two paradigms. Increasing γ tightens the effective timing window for block proposal, as a larger fraction of attesters must be reached before the consensus deadline, thereby increasing the role of latency.

Under external block building, this amplifies migration incentives. Since block dissemination is handled by the supplier, the proposer’s location affects only the freshness of the supplier’s offered value. As the effective timing window shrinks, reducing proposer–supplier latency yields a larger marginal increase in attainable block value, making migration toward the supplier more attractive.

Under local block building, by contrast, higher attestation thresholds dampen migration incentives. Because proposer location affects both value accrual and timely block dissemination, proposers face a sharper trade-off between remaining close enough to attesters to satisfy the quorum and remaining close to multiple information sources to maximize aggregate block value. At lower thresholds, fewer attesters need to be reached, allowing validators to prioritize information-source proximity and migrate toward dominant hubs. Higher thresholds force a more balanced consideration of these two dimensions, reducing the benefit of migrating toward any single region.

Overall, these results show that the impact of the attestation threshold on migration incentives depends critically on the adopted block-building paradigm, as γ alters the relative importance of propagation latency and information aggregation in proposers’ location decisions.

4.6.2 Shorter Slot Time Effect. We analyze how changing the consensus slot time Δ affects validators’ migration incentives. Motivated by recent community discussions surrounding Ethereum Improvement Proposal (EIP)-7782 [1], which proposes reducing the slot time from $\Delta = 12$ s to $\Delta = 6$ s with an earlier attestation deadline of $\tau_{\text{cut}} = 3$ s, we halve the slot time and shift the attestation deadline accordingly in our simulations. The stated goals of this proposal are increased throughput and improved user experience. Recent empirical measurements [47] report sub-second block propagation times, suggesting that such shorter slot durations may be feasible in practice.

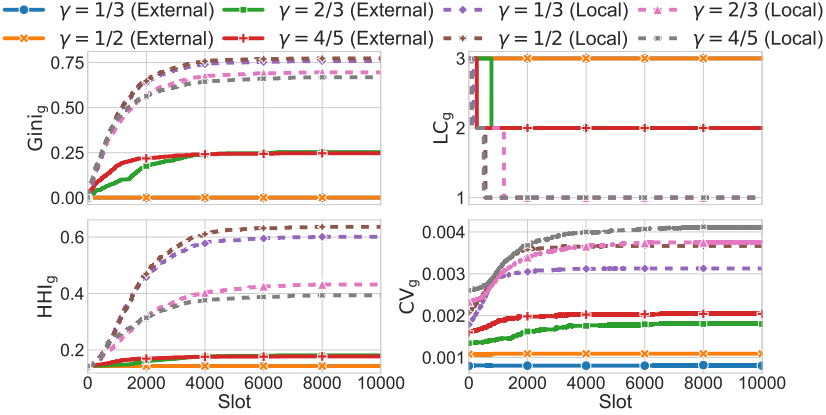


Fig. 7. *Attestation-threshold effect (homogeneous validators and information sources)*. Evolution of centralization metrics under Local and External block-building paradigms for different attestation thresholds $\gamma \in \{\frac{1}{3}, \frac{1}{2}, \frac{2}{3}, \frac{4}{5}\}$.

Figure 8 shows the evolution of our metrics under a 6 s slot time, alongside the baseline 12 s configuration. Because observed propagation delays are small relative to the shortened timing window, proposers face essentially the same co-location trade-offs as under $\Delta = 12$ s. As a result, the trajectories of the centralization indices and the liveness coefficient remain largely unchanged across both block-building paradigms, consistent with empirical observations in [47].

We do, however, observe higher reward variance across regions under $\Delta = 6$ s for both paradigms. This arises because latency advantages are effectively absolute: when the slot duration is shorter, a fixed latency edge constitutes a larger fraction of the available timing window. Consequently, the same latency differential yields a larger relative payoff advantage, amplifying cross-regional reward disparities.

Overall, these results show that halving the slot time does not materially affect geographical centralization under either block-building paradigm. However, as the relative importance of latency increases, reward disparities across regions become more pronounced, suggesting that beyond a certain threshold, further reductions in slot time may begin to strengthen migration incentives.

5 Discussion

In this section, we discuss the implications of our simulation results, outline how our findings can inform potential mitigation strategies, and acknowledge the limitations of our framework.

5.1 Implications

Our results indicate that Ethereum’s block-building architecture is *not* geographically neutral and systematically shapes validators’ migration incentives. Across all experiments, we observe that both local and external block-building paradigms induce location-dependent payoffs, albeit through different mechanisms. While externalizing block building via PBS/ePBS decouples block propagation from proposer location, it introduces new incentives to co-locate with suppliers, making supplier geography a central determinant of validator positioning.

More broadly, our findings indicate that information-source placement and supplier location are first-order protocol considerations rather than mere infrastructural artifacts. As shown across heterogeneous source and validator configurations, asymmetries in access to information or block

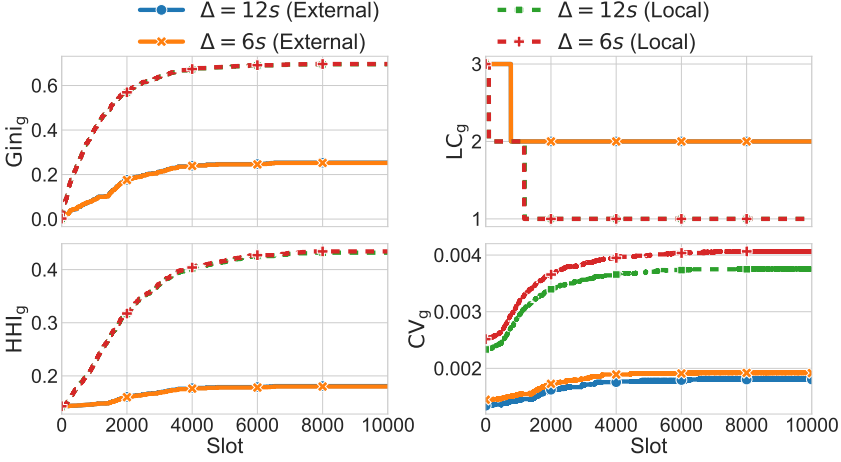


Fig. 8. *Shorter slot time effect (homogeneous validators and information sources)*. Evolution of centralization metrics under Local and External block-building paradigms with a shorter slot time ($\Delta = 6$ s) versus the current slot time ($\Delta = 12$ s).

suppliers consistently amplify migration incentives and accelerate geographical concentration, even when validators begin from a balanced distribution.

Finally, consensus parameters act as incentive amplifiers by modulating latency sensitivity. Changes to attestation thresholds and slot times do not uniformly affect centralization outcomes, but they alter which latency components dominate proposers’ payoff calculations. As a result, seemingly orthogonal protocol choices—such as quorum requirements or slot duration—can materially influence geographical positioning incentives.

Taken together, these results imply that protocol designers and infrastructure operators must treat geography as an endogenous outcome of protocol design. Ignoring these incentive effects risks undermining decentralization, liveness, and censorship resistance, even in the absence of explicit coordination among validators.

5.2 Mitigations

The mechanisms identified in our analysis point to several potential directions for mitigating geographical centralization at both the protocol and infrastructure levels. A key driver of migration incentives in our analysis is the deterministic selection of a single proposer under Ethereum’s PoS, which grants the proposer temporary monopoly power over block release and enables timing games. Our simulations confirm that this monopoly incentivizes validators to reduce latency in order to extend their effective proposal window, thereby increasing attainable rewards.

One potential mitigation is to weaken the monopoly power of a single proposer through decentralized block-building networks such as BuilderNet [7] and Multiple Concurrent Proposers (MCP) designs [25, 41], in which multiple entities contribute block content within a single slot. However, these protocols may introduce new strategic positioning incentives, as participants seek preferential access to exclusive order flow or content sources, implying a trade-off rather than a definitive remedy.

A complementary mitigation direction operates at the incentive level by reducing the sensitivity of validator rewards to marginal latency advantages. Mechanisms such as *MEV-burn* [18] dampen the payoff differences arising from timing games, thereby weakening the economic incentive to migrate

for latency advantages. While such mechanisms are primarily motivated by economic fairness, our results suggest they may also reduce geographically driven concentration by decoupling reward access from physical proximity.

Finally, our findings indicate that supplier geography [16] itself becomes a critical determinant of validator positioning under external block building. This suggests that encouraging geographical diversity among builders, relays, or other block suppliers, as well as among major applications that act as signal sources—whether through governance norms, transparency requirements, or explicit protocol incentives—could mitigate the concentration pressures we observe. More broadly, treating geographical decentralization as an explicit protocol objective, rather than an emergent property, may help prevent the long-term erosion of Ethereum’s security assumptions.

5.3 Limitations

Latency data. Our simulations rely on latency and regional information derived from GCP data. This choice provides a consistent, publicly available, and well-documented dataset, making the analysis transparent and reproducible. Nevertheless, it may introduce bias: other cloud service providers may offer denser regional coverage or slightly lower inter-region latency, potentially affecting validator connectivity and block propagation dynamics, and thus the quantitative outcomes of our simulations.

That said, major providers such as AWS, Azure, and OVH, exhibit broadly similar regional distributions [2, 39, 42], with most regions concentrated in Europe, North America, and Asia. Moreover, since inter-regional latencies are largely determined by underlying fiber-optic infrastructure, using data from alternative providers would likely yield comparable results. As future work, we plan to use datasets from other providers to further validate our findings.

Value function. We model block value as a deterministic function that increases monotonically over time. This abstraction is chosen to isolate proposer timing and migration incentives while ensuring tractable analysis. However, it omits stochastic effects present in practice, such as random transaction arrivals, volatile MEV opportunities, or builder-specific bidding dynamics. Under the local block-building paradigm, we further assume that signals from different information sources are additive. In practice, such signals may overlap, and their joint contribution to the block value would depend on their interaction structure, which we do not model. Finally, we treat information sources as fungible with identical value parameters, whereas in practice, suppliers and signal sources may differ substantially in the value they provide.

Information assumptions. Our framework assumes that proposers have sufficiently accurate information to evaluate their decisions, including expected propagation delays across regions and expected value differences between locations. This corresponds to a full-information benchmark that allows us to characterize proposers’ best-response behaviors in an interpretable manner.

In practice, such information is often only available at coarse granularity. Expected values depend on stochastic market dynamics, and validators may have limited visibility into the geographical distribution of other validators, constraining their ability to form precise expectations about propagation delays. Imperfect information would primarily affect the speed and path of adjustment rather than the existence of incentives themselves. With noisy estimates, proposer behavior can be interpreted as perturbed best responses, leading to slower convergence and occasional mis-relocations, but not eliminating the underlying latency- and value-driven incentives identified in our analysis.

Migration. We assume that validator migration occurs instantaneously and at a constant cost. This assumption represents a best-case scenario and allows us to focus on long-run location incentives rather than short-run adjustment frictions. It is motivated by the fact that validators

can anticipate proposer duties and pre-synchronize infrastructure in target regions, making near-instant switchover feasible in some settings. In practice, however, migration costs and delays may vary depending on technical frictions, cloud-provider pricing, or operational risk. Modeling heterogeneous and time-varying migration processes is an important direction for future work.

6 Related Work

Blockchain decentralization. Prior work has measured (de)centralization using diverse metrics. The Nakamoto coefficient was introduced to capture the minimum number of entities needed to compromise a blockchain subsystem [48]. Other measures, including the Gini coefficient [17], Shannon entropy [36], and the Herfindahl–Hirschman index [45], have been applied to quantify (de)centralization in various contexts, such as mining power [35, 37, 58], staking distribution [28, 35], and block building [29, 44, 59]. Our work examines a different dimension by proposing metrics that capture the geographical distribution of validators.

Geographical location of Ethereum validators. Validators’ geo-location has received less attention despite its importance for latency and fault tolerance. Kim et al. developed NodeFinder to measure Ethereum Peer-to-Peer (P2P) networks during the Proof-of-Work (PoW) era, finding that as of 2018, most nodes were in the U.S. (43.2%), China (12.9%), and Germany (5.2%) [33]. Similar inference methods have been applied to the PoS era [6], showing continued concentration in a few countries. Online dashboards [10, 22] report real-time Ethereum node distribution and, as of December 2025, identify the United States and Germany as dominant. Heimbach et al. further developed a deanonymization technique that located over 15% of validators, with more than 85% situated in Europe and North America [30]. Kiffer et al. measured the P2P infrastructure of 36 public blockchain networks, including Ethereum, and found that node deployment is highly geographically concentrated, with most nodes located in the United States and Western Europe [32].

ABM in blockchain. ABM has been widely adopted to model the strategic behavior of blockchain participants. Kraner et al. modeled Ethereum PoS to analyze how network topology and latency influence consensus performance and stability [34]. Öz et al. examined the impact of waiting games on consensus stability, showing that delay strategies can be profitable without undermining consensus when widely adopted [43]. Other works used ABM to study builder behaviors in MEV-Boost auctions [56, 57], assess design proposals such as Execution Tickets [49], and analyze how staking and inflation policies shape token concentration in DAO and DeFi governance [12].

7 Conclusion

In this paper, we design and implement an agent-based simulation framework to study how Ethereum’s protocol design—particularly its block-building paradigms of local and external block building—interacts with validator and information-source distributions to shape geographical positioning incentives. Through controlled simulations, we show that Ethereum’s block-building architecture is not geographically neutral: both paradigms induce location-dependent payoffs and migration incentives, with asymmetric access to information sources and suppliers amplifying geographical centralization.

We further demonstrate that consensus parameters, such as attestation thresholds and slot times, modulate latency sensitivity and can act as protocol-level levers that amplify or dampen these effects. Together, our results highlight that geographical decentralization is an emergent outcome of protocol design choices rather than a purely infrastructural concern. Finally, we discuss the implications of these findings for ongoing protocol evolution and outline potential mitigation directions aimed at preserving Ethereum’s decentralization and security properties.

Acknowledgments

The authors appreciate Quintus Kilbourn, Lioba Heimbach, Thomas Thiery, Devan Mitchem, Akaki Mamageishvili, István András Seres, Bruno Mazorra, Christoph Schlegel, and Luis Correia for helpful discussions and comments. Fei Wu acknowledges support from a Flashbots research grant.

References

- [1] Ben Adams and Dankrad Feist. 2024. EIP-7782: Reduce Block Latency [DRAFT]. *Ethereum Improvement Proposals 7782* (October 2024). <https://eips.ethereum.org/EIPS/eip-7782> [Online serial].
- [2] Amazon Web Services, Inc. 2025. AWS Global Infrastructure. <https://aws.amazon.com/about-aws/global-infrastructure/>. Accessed: 2025-09-17.
- [3] Authors. 2025. Geographical Decentralization Simulation. <https://geo-decentralization.github.io/>.
- [4] Authors. 2025. geographical-decentralization-simulation. <https://github.com/syang-ng/geographical-decentralization-simulation> Accessed: 2025-12-28.
- [5] Blockchain.com. 2025. Hashrate Distribution (Pools). <https://www.blockchain.com/explorer/charts/pools>. Accessed: 2025-09-09.
- [6] Jonas Bostoen and Naman Garg. 2024. Estimating Validator Decentralization Using p2p Data. <https://ethresear.ch/t/estimating-validator-decentralization-using-p2p-data/19920>.
- [7] BuilderNet. 2025. Welcome to BuilderNet. <https://buildernet.org/docs>
- [8] Vitalik Buterin. 2025. Comment on protocol security and attestation thresholds. <https://x.com/VitalikButerin/status/1993439679081857433>. X (formerly Twitter) post.
- [9] Vitalik Buterin, Diego Hernandez, Thor Kampefner, Khiem Pham, Zhi Qiao, Danny Ryan, Juhyeok Sin, Ying Wang, and Yan X Zhang. 2020. Combining ghost and casper. *arXiv preprint arXiv:2003.03052* (2020).
- [10] Cambridge Centre for Alternative Finance (CCAF). 2025. Ethereum Network Analytics. https://ccaf.io/cbnsi/ethereum/network_analytics. Accessed September 1, 2025.
- [11] Chainbound. 2024. Geolocating Validators. <https://dune.com/chainbound/geolocating-validators>. Accessed: 2025-08-18.
- [12] Lin William Cong, Yilei Dong, Yunbo Lu, Qingsong Ruan, and Guojun Wang. 2024. Agent-Based Modeling for DAOs and DeFi. *Available at SSRN 5171559* (2024).
- [13] Lin William Cong, Zhiguo He, and Jiasun Li. 2021. Decentralized mining in centralized pools. *The Review of Financial Studies* 34, 3 (2021), 1191–1235.
- [14] Philip Daian, Steven Goldfeder, Tyler Kell, Yunqi Li, Xueyuan Zhao, Iddo Bentov, Lorenz Breidenbach, and Ari Juels. 2020. Flash Boys 2.0: Frontrunning in Decentralized Exchanges, Miner Extractable Value, and Consensus Instability. In *2020 IEEE symposium on security and privacy (SP)*. IEEE Computer Society, Los Alamitos, CA, USA, 910–927.
- [15] DataAlways. 2025. The Block Auction Infrastructure Race. <https://collective.flashbots.net/t/the-block-auction-infrastructure-race/4734>
- [16] DataAlways. 2025. The Geography of Block Building. <https://collective.flashbots.net/t/the-geography-of-block-building/5367/1>
- [17] Robert Dorfman. 1979. A Formula for the Gini Coefficient. *The review of economics and statistics* (1979), 146–149.
- [18] Justing Drake. 2023. MEV-Burn: A Simple Design. <https://ethresear.ch/t/mev-burn-a-simple-design/15590>.
- [19] Ethereum Foundation. 2024. Proposer-Builder Separation. <https://ethereum.org/en/roadmap/pbs/>. Accessed: 2025-08-13.
- [20] Ethereum Foundation. 2025. Ethereum Proof-of-Stake Consensus Specifications. <https://github.com/ethereum/consensus-specs>. Accessed: 2025-09-09.
- [21] Ethereum Foundation. 2025. The Merge. <https://ethereum.org/en/roadmap/merge/>.
- [22] ethernodes.org. 2025. Ethernodes – Countries. <https://www.ethernodes.org/countries>. Accessed: 2025-09-01.
- [23] Flashbots. 2025. Overview – MEV-Boost. <https://docs.flashbots.net/flashbots-mev-boost/introduction>. Accessed: 2025-08-03.
- [24] Francesco D’Amato and Barnabé Monnot and Michael Neuder and Potuz and Terence Tsao. 2024. EIP-7732: Enshrined Proposer-Builder Separation. <https://eips.ethereum.org/EIPS/eip-7732>. Accessed: 2025-12-24.
- [25] Pranav Garimidi, Joachim Neu, and Max Resnick. 2025. Multiple Concurrent Proposers: Why and How. <https://eprint.iacr.org/2025/1772> Publication info: Preprint..
- [26] Adem Efe Gencer, Soumya Basu, Ittay Eyal, Robbert Van Renesse, and Emin Gün Sirer. 2018. Decentralization in bitcoin and ethereum networks. In *International conference on financial cryptography and data security*. Springer, Springer-Verlag, Berlin, Heidelberg, 439–457. doi:10.1007/978-3-662-58387-6_24
- [27] Google. 2025. Google Looker Studio Dashboard: fc733b10-9744-4a72-a502-92290f608571. <https://lookerstudio.google.com/reporting/fc733b10-9744-4a72-a502-92290f608571>. Accessed: 2025-09-11.

- [28] Dominic Grandjean, Lioba Heimbach, and Roger Wattenhofer. 2024. Ethereum Proof-of-Stake Consensus Layer: Participation and Decentralization. In *International Conference on Financial Cryptography and Data Security*. Springer, Springer-Verlag, Berlin, Heidelberg, 253–280. doi:10.1007/978-3-031-69231-4_17
- [29] Lioba Heimbach, Lucianna Kiffer, Christof Ferreira Torres, and Roger Wattenhofer. 2023. Ethereum’s Proposer-Builder Separation: Promises and Realities. In *2023 ACM Internet Measurement Conference (IMC), Montreal, QC, Canada*. Association for Computing Machinery, New York, NY, USA, 406–420. doi:10.1145/3618257.3624824
- [30] Lioba Heimbach, Yann Vonlanthen, Juan Villacis, Lucianna Kiffer, and Roger Wattenhofer. 2025. Deanonymizing Ethereum Validators: The P2P Network Has a Privacy Issue. In *34th USENIX Security Symposium*. USENIX Association, Seattle, WA, USA.
- [31] Harold Hotelling. 1929. Stability in Competition. *The Economic Journal* 39, 153 (1929), 41–57. doi:10.2307/2224214
- [32] Lucianna Kiffer, Lioba Heimbach, Dennis Trautwein, Yann Vonlanthen, and Oliver Gasser. 2025. Multiple Sides of 36 Coins: Measuring Peer-to-Peer Infrastructure Across Cryptocurrencies. *Proceedings of the ACM on Measurement and Analysis of Computing Systems* 9, 3 (2025), 1–32.
- [33] Seoung Kyun Kim, Zane Ma, Siddharth Murali, Joshua Mason, Andrew Miller, and Michael Bailey. 2018. Measuring ethereum network peers. In *Proceedings of the Internet Measurement Conference 2018*. Association for Computing Machinery, New York, NY, USA, 91–104. doi:10.1145/3278532.3278542
- [34] Benjamin Kraner, Nicolò Vallarano, Caspar Schwarz-Schilling, and Claudio J Tessone. 2023. Agent-based modelling of ethereum consensus. In *2023 IEEE International Conference on Blockchain and Cryptocurrency (ICBC)*. IEEE, IEEE Computer Society, Los Alamitos, CA, USA, 1–8. doi:10.1109/ICBC56567.2023.10174948
- [35] Yujin Kwon, Jian Liu, Minjeong Kim, Dawn Song, and Yongdae Kim. 2019. Impossibility of Full Decentralization in Permissionless Blockchains. In *Proceedings of the 1st Conference on Advances in Financial Technologies (AFT)*. Association for Computing Machinery, New York, NY, USA, 110–123. doi:10.1145/3318041.3355463
- [36] Jianhua Lin. 1991. Divergence Measures Based on the Shannon Entropy. *IEEE Transactions on Information Theory* 37, 1 (1991), 145–151.
- [37] Qinwei Lin, Chao Li, Xifeng Zhao, and Xianhai Chen. 2021. Measuring Decentralization in Bitcoin and Ethereum using Multiple Metrics and Granularities. In *2021 IEEE 37th International Conference on Data Engineering Workshops (ICDEW)*. IEEE, IEEE Computer Society, Los Alamitos, CA, USA, 80–87. doi:10.1109/ICDEW53142.2021.00022
- [38] Charles M Macal and Michael J North. 2005. Tutorial on agent-based modeling and simulation. In *Proceedings of the Winter Simulation Conference, 2005*. IEEE, Winter Simulation Conference, Orlando, Florida, 14–pp.
- [39] Microsoft Corporation. 2025. Azure Regions List. <https://learn.microsoft.com/en-us/azure/reliability/regions-list>. Accessed: 2025-09-17.
- [40] Satoshi Nakamoto. 2008. Bitcoin: A peer-to-peer electronic cash system. Available at SSRN 3440802 (2008).
- [41] Mike Neuder and Max Resnick. 2024. Concurrent Block Proposers in Ethereum. <https://ethresear.ch/t/concurrent-block-proposers-in-ethereum/18777>.
- [42] OVHcloud. 2025. OVHcloud Locations: Global Infrastructure Locations. <https://us.ovhcloud.com/about/global-infrastructure/locations/>. Accessed: 2025-09-17.
- [43] Burak Öz, Benjamin Kraner, Nicolò Vallarano, Bingle Stegmann Kruger, Florian Matthes, and Claudio Juan Tessone. 2023. Time Moves Faster When There is Nothing You Anticipate: The Role of Time in MEV Rewards. In *Proceedings of the 2023 Workshop on Decentralized Finance and Security (Copenhagen, Denmark) (DeFi '23)*. Association for Computing Machinery, New York, NY, USA, 1–8. doi:10.1145/3605768.3623563
- [44] Burak Öz, Danning Sui, Thomas Thiery, and Florian Matthes. 2024. Who Wins Ethereum Block Building Auctions and Why?. In *6th Conference on Advances in Financial Technologies (Leibniz International Proceedings in Informatics (LIPIcs), Vol. 316)*. Schloss Dagstuhl – Leibniz-Zentrum für Informatik, Dagstuhl, Germany, 22:1–22:25. doi:10.4230/LIPIcs.AFT.2024.22
- [45] Stephen A Rhoades. 1993. The Herfindahl–Hirschman Index. *Fed. Res. Bull.* 79 (1993), 188.
- [46] Caspar Schwarz-Schilling, Fahad Saleh, Thomas Thiery, Jennifer Pan, Nihar Shah, and Barnabé Monnot. 2023. Time Is Money: Strategic Timing Games in Proof-Of-Stake Protocols. In *5th Conference on Advances in Financial Technologies (AFT 2023) (Leibniz International Proceedings in Informatics (LIPIcs), Vol. 282)*. Schloss Dagstuhl – Leibniz-Zentrum für Informatik, Dagstuhl, Germany, 30:1–30:17. doi:10.4230/LIPIcs.AFT.2023.30
- [47] Maria Inês Silva. 2025. An analysis of attestation timings in a 6-s slot. <https://ethresear.ch/t/an-analysis-of-attestation-timings-in-a-6-s-slot/23016>.
- [48] Balaji S Srinivasan and Leland Lee. 2017. Quantifying Decentralization. *news.earn.com* (2017).
- [49] Pascal Stichler. 2025. Galaxy Era: Agent-based Simulation of Execution Tickets. *arXiv preprint arXiv:2501.16090* (2025).
- [50] Ewout ter Hoeven, Jan Kwakkel, Vincent Hess, Thomas Pike, Boyu Wang, Jackie Kazil, et al. 2025. Mesa 3: Agent-based modeling with Python in 2025. *Journal of Open Source Software* 10, 107 (2025), 7668.
- [51] Alex Thorn, Amanda Fabiano, and Karim Helmy. 2021. Examining the Latest China Bitcoin Ban. <https://www.galaxy.com/insights/research/examining-the-latest-china-bitcoin-ban> Research article.

- [52] Anton Wahrstätter, Jens Ernstberger, Aviv Yaish, Liyi Zhou, Kaihua Qin, Taro Tsuchiya, Sebastian Steinhorst, Davor Svetinovic, Nicolas Christin, Mikolaj Barczentewicz, et al. 2024. Blockchain Censorship. In *Proceedings of the ACM Web Conference 2024*. Association for Computing Machinery, New York, NY, USA, 1632–1643. doi:10.1145/3589334.3645431
- [53] Anton Wahrstätter, Liyi Zhou, Kaihua Qin, Davor Svetinovic, and Arthur Gervais. 2023. Time to bribe: Measuring block construction market. *arXiv preprint arXiv:2305.16468* (2023).
- [54] Toni Wahrstätter. 2024. Is it Worth Using MEV-Boost? <https://ethresear.ch/t/is-it-worth-using-mev-boost/19753>. Accessed: 2026-01-05.
- [55] Fei Wu, Danning Sui, Thomas Thiery, and Mallesh Pai. 2025. Measuring CEX-DEX Extracted Value and Searcher Profitability: The Darkest of the MEV Dark Forest. In *7th Conference on Advances in Financial Technologies (AFT 2025) (Leibniz International Proceedings in Informatics (LIPIcs), Vol. 354)*, Zeta Avarikioti and Nicolas Christin (Eds.), Schloss Dagstuhl – Leibniz-Zentrum für Informatik, Dagstuhl, Germany, 26:1–26:23. doi:10.4230/LIPIcs.AFT.2025.26
- [56] Fei Wu, Thomas Thiery, Stefanos Leonardos, and Carmine Ventre. 2024. Strategic bidding wars in on-chain auctions. In *2024 IEEE International Conference on Blockchain and Cryptocurrency (ICBC)*. IEEE, IEEE Computer Society, Los Alamitos, CA, USA, 503–511.
- [57] Fei Wu, Thomas Thiery, Stefanos Leonardos, and Carmine Ventre. 2025. From Competition to Centralization: The Oligopoly in Ethereum Block Building Auctions. In *ECAI 2025 - 28th European Conference on Artificial Intelligence, including 14th Conference on Prestigious Applications of Intelligent Systems, PAIS 2025 - Proceedings (Frontiers in Artificial Intelligence and Applications)*, 3387–3394. doi:10.3233/FAIA251209
- [58] Keke Wu, Bo Peng, Hua Xie, and Zhen Huang. 2019. An Information Entropy Method to Quantify the Degrees of Decentralization for Blockchain Systems. In *2019 IEEE 9th International Conference on Electronics Information and Emergency Communication (ICEIEC)*. IEEE, IEEE Computer Society, Los Alamitos, CA, USA, 1–6.
- [59] Sen Yang, Kartik Nayak, and Fan Zhang. 2025. Decentralization of Ethereum's Builder Market. In *2025 IEEE Symposium on Security and Privacy (SP)*. IEEE, IEEE Computer Society, Los Alamitos, CA, USA, 1512–1530. doi:10.1109/SP61157.2025.00157

A List of Google Cloud Platform Regions

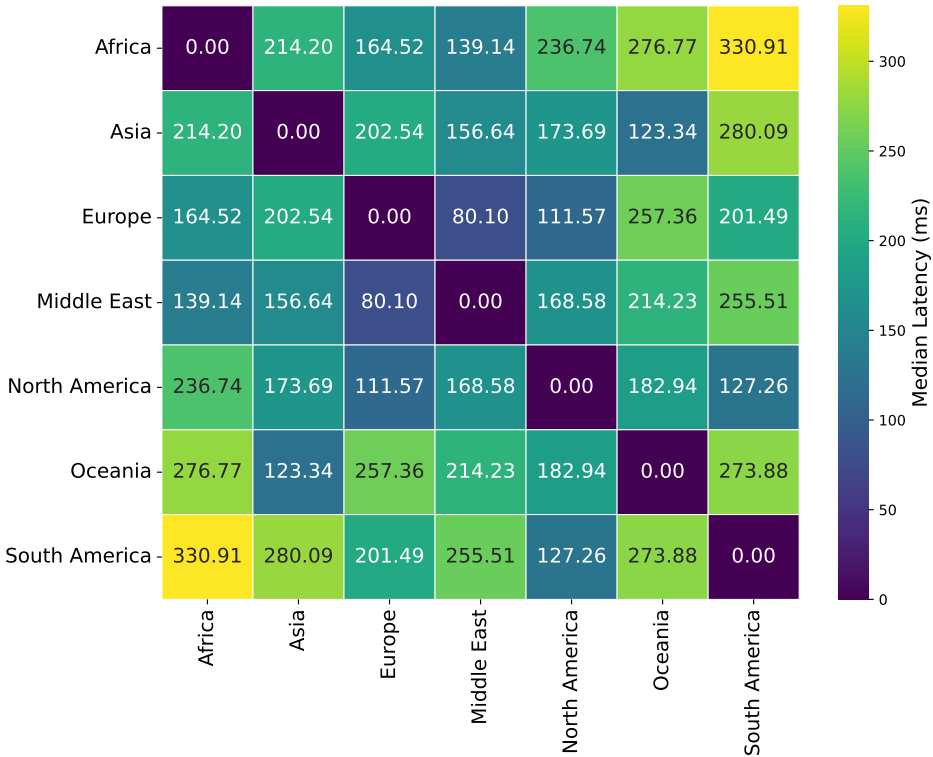


Fig. 9. Heatmap of median latency between macro-regions.

In this section, we present the list of Google Cloud Platform (GCP) regions used in our paper, along with their physical locations, as shown in Table 1. We exclude two GCP regions—me-central2 (Dammam, Saudi Arabia) and northamerica-south1 (Queretaro, Mexico)—because latency data between these regions and the others was not available [27].

Figure 9 presents the heatmap of median latency between each pair of macro-regions. For example, the median latency between Asia and Europe is computed as the median value of all latencies between GCP regions in Asia and GCP regions in Europe. Among the seven macro-regions, North America has the best average median latency to other regions (142.97 ms), while South America has the worst (209.88 ms).

Table 1. GCP regions and their physical locations.

Macro-Region	GCP Region	Location
Africa	africa-south1	Johannesburg, South Africa
Asia	asia-east1	Changhua County, Taiwan
	asia-east2	Hong Kong, China
	asia-northeast1	Tokyo, Japan
	asia-northeast2	Osaka, Japan
	asia-northeast3	Seoul, South Korea
	asia-south1	Mumbai, India
	asia-south2	Delhi, India
	asia-southeast1	Singapore
Oceania	asia-southeast2	Jakarta, Indonesia
	australia-southeast1	Sydney, Australia
Europe	australia-southeast2	Melbourne, Australia
	euope-central2	Warsaw, Poland
	euope-north1	Hamina, Finland
	euope-north2	Stockholm, Sweden
	euope-southwest1	Madrid, Spain
	euope-west1	St. Ghislain, Belgium
	euope-west2	London, UK
	euope-west3	Frankfurt, Germany
	euope-west4	Eemshaven, Netherlands
	euope-west6	Zurich, Switzerland
	euope-west8	Milan, Italy
	euope-west9	Paris, France
euope-west10	Berlin, Germany	
euope-west12	Turin, Italy	
Middle East	me-central1	Doha, Qatar
	me-west1	Tel Aviv, Israel
South America	southamerica-east1	Sao Paulo, Brazil
	southamerica-west1	Santiago, Chile
North America	northamerica-northeast1	Montreal, Canada
	northamerica-northeast2	Toronto, Canada
	us-central1	Council Bluffs, Iowa, USA
	us-east1	Moncks Corner, SC, USA
	us-east4	Ashburn, Virginia, USA
	us-east5	Columbus, Ohio, USA
	us-south1	Dallas, Texas, USA
	us-west1	The Dalles, Oregon, USA
	us-west2	Los Angeles, California, USA
	us-west3	Salt Lake City, Utah, USA
us-west4	Las Vegas, Nevada, USA	

B List of Symbols

Table 2. List of symbols.

Symbol	Description
Geography and Latency	
$\mathcal{R} = \{r_1, \dots, r_m\}$	Set of geographical regions
$d(r_j, r_k)$	Message propagation latency from region r_j to r_k , drawn from a log-normal distribution
μ_{jk}	Mean of $\ln d(r_j, r_k)$
Validators and Consensus	
$\mathcal{V} = \{v_1, \dots, v_P\}$	Set of validators (agents)
n	Slot index, $n \in \{1, \dots, N\}$
p_n	Proposer selected for slot n
$r(p_n)$	Region of the proposer of slot n
$a \in \mathcal{A}_n$	An attester in the set of attestors assigned to slot n
$r(a)$	Region of attester a
γ	Fraction of attestation required for canonicalization
Δ	Slot duration
τ	Block release time within a slot
τ_{cut}	Cutoff time for timely attestations
c	Cost of migration across regions
Information Sources	
\mathcal{I}	Set of information sources
$\mathcal{I}_{\text{signal}}$	Set of signal sources (used in the local block building paradigm)
$\mathcal{I}_{\text{supplier}}$	Set of block suppliers (used in the external block building paradigm)
$r(I)$	Region of signal source or block supplier I
$V_I(t) = a_I t + b_I$	Value available from source or supplier I at time t
$V_r(\tau)$	Aggregate block value for a proposer located in region r at release time τ
Attestation and Payoffs	
$q_a(\tau; r)$	Probability that attester a votes on time when a block is released at (r, τ)
$S(\tau; r)$	Number of timely attestations for a block released at (r, τ)
$\Pi_r(\tau)$	Probability that a block released at (r, τ) becomes canonical
τ_r^*	Optimal block release time for a proposer in region r
$W(r)$	Expected payoff for a proposer located in region r
τ_I^*	Optimal release time when using block supplier I
$W(I)$	Expected payoff when using block supplier I
\mathcal{W}	Set of best expected proposer payoffs across regions in a slot

C Marginal Benefit Distribution

Figure 10 shows the CDF of marginal benefits when proposers move to the best region during the first 1,000 slots under the baseline configuration with migration cost $c = 0$, in which both validators

and information sources are uniformly distributed across macro-regions and evenly within each macro-region’s GCP regions. Under the external block-building paradigm, about 80% of migration marginal benefits are less than 0.002, which suggests that such migration could be prevented if the migration cost is 0.002.

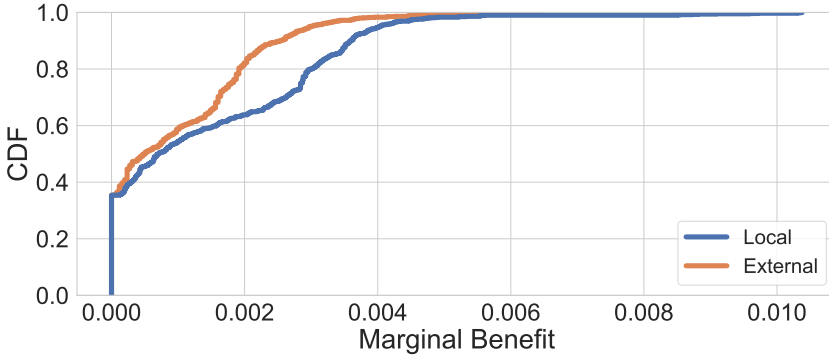


Fig. 10. CDF of marginal benefit in the first 1,000 slots under the baseline configuration.

D Experiments with Different Scales

We evaluated whether our results are sensitive to the scale of the simulation by running the same experiment (with homogeneous validators and information sources, and $c = 0$) under three configurations: $|\mathcal{V}| = 100$ validators with $N = 1,000$ slots; $|\mathcal{V}| = 1,000$ validators with $N = 10,000$ slots; and $|\mathcal{V}| = 10,000$ validators with $N = 100,000$ slots.

While the absolute values of the per-slot metrics differ across scales, this is largely due to the different slot horizons. As shown in Figure 11, when we normalize time by the normalized relative progress within an experiment (i.e., the current slot index divided by the total number of slots), the trajectories align closely and exhibit the same qualitative trends across all three configurations.

We observe that the CV_g exhibits slightly larger differences across scales compared to the other centralization metrics. This is mainly driven by our latency model, in which the probability that a block becomes canonical depends on a Poisson–binomial tail probability over timely attestations. When the attester (validator) population is small (e.g., $|\mathcal{V}| = 100$), this Poisson–binomial aggregation exhibits stronger finite-size effects, so small differences in per-attester latency probabilities $q_a(\tau; r)$ translate into more visible differences in $\Pi_r(\tau)$ and, consequently, the resulting per-slot outcomes. As the system scales to $|\mathcal{V}| = 1,000$ and 10,000, this aggregation concentrates and the effect diminishes. Importantly, despite these scale-dependent differences in absolute CV_g values, the relative ordering, temporal evolution, and overall qualitative trends remain consistent across all configurations, indicating that our conclusions are driven by the underlying dynamics rather than a particular system scale.

Simulations with larger validator populations are substantially more expensive. For $|\mathcal{V}| = 10,000$, the runtime of a single-slot simulation already exceeds one second, making a full simulation with $N = 100,000$ slots take more than a day to complete. We therefore adopt $|\mathcal{V}| = 1,000$ for most experiments in this paper, as it provides a practical balance between computational feasibility and statistical stability while preserving the same trends observed at larger scales.

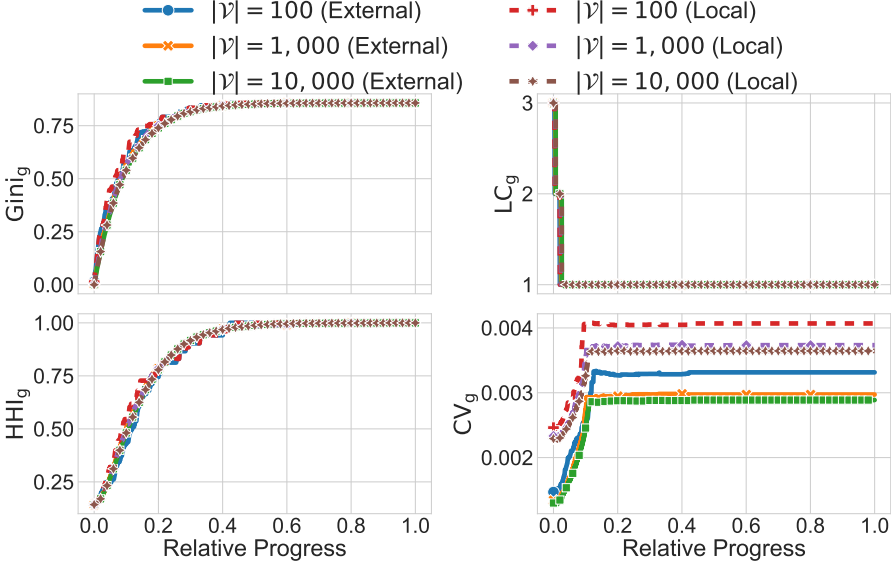


Fig. 11. *Setup: Homogeneous validators and information sources with $c = 0$.* Evolution of centralization metrics under Local and External block-building paradigms across different system scales, with $(|\mathcal{V}|, N) \in (100, 1,000), (1,000, 10,000), (10,000, 100,000)$. The x-axis shows normalized progress, defined as the current slot index divided by the total number of slots.

E Migration Costs

We evaluate how migration costs affect both the degree and speed of geographical centralization. Using the baseline configuration in Section 4.2 (homogeneous validators and information sources), we vary the cost from 0 to 0.003; at the upper end of this range, the cost removes over 70% of the typical marginal relocation gain in both the local and external block-building paradigms (see Figure 10). As shown in Figure 12, higher costs predictably dampen validator mobility and mitigate centralization. This migration-suppressing effect is consistently stronger under the external block-building paradigm than under the local block-building paradigm, reflecting Section 4.2: under the local block-building paradigm, location directly shifts marginal value via multi-source aggregation, sustaining stronger incentives to co-locate even when migration is costly.

F Baseline Configuration: Validator Convergence Locus

Figure 13 illustrates how validators redistribute across macro-regions over time in the baseline simulation of Section 4.2, starting from an initially uniform geographical distribution. This visualization highlights not only the overall degree of centralization but also *where* validators ultimately converge, providing insight into which regions offer systematic advantages.

Under the external block-building paradigm, migration yields only modest gains, as discussed in Section 4.2. A small fraction of validators initially relocates to North America, slightly altering the validator distribution. This shift not only benefits validators in North America but also alters the attester distribution, indirectly improving supplier–attester latency for other macro-regions. Owing to its geographic position, the Middle East exhibits relatively low average latency to multiple macro-regions (see Figure 9) and thus gains a slight relative advantage as the distribution evolves.

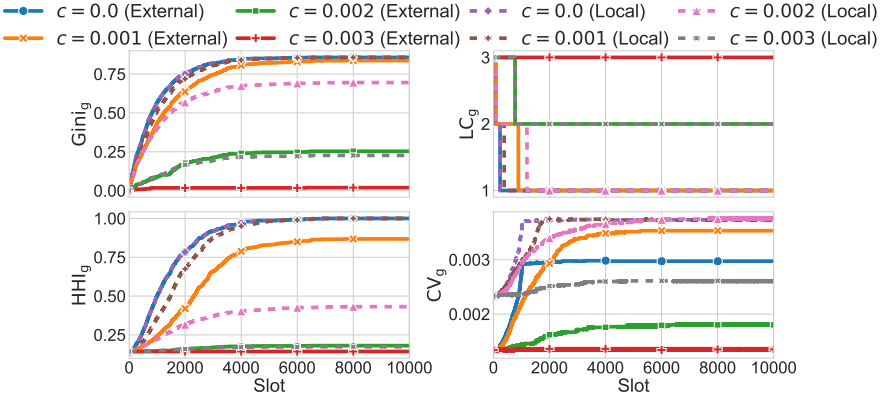


Fig. 12. *Setup: Homogeneous validators and information sources.* Evolution of centralization metrics under Local and External block-building paradigms with varying migration costs $c \in \{0, 0.001, 0.002, 0.003\}$.

As a result, validators initially located in South America tend to relocate to the Middle East, while most other regions experience weak migration incentives and largely retain their initial shares.

Under the local block-building paradigm, migration incentives are stronger because validator location directly affects both value accumulation and propagation to attesters. Validators initially migrate toward North America, where early concentration forms. As this concentration increases, validators located in South America and Africa gradually find it more profitable to relocate to Europe, reflecting Europe’s relatively low latency to the emerging North American hub. This secondary migration induces further concentration in Europe through network effects. Migration costs, however, prevent full convergence, leaving a non-trivial fraction of validators remaining in North America and the Middle East.

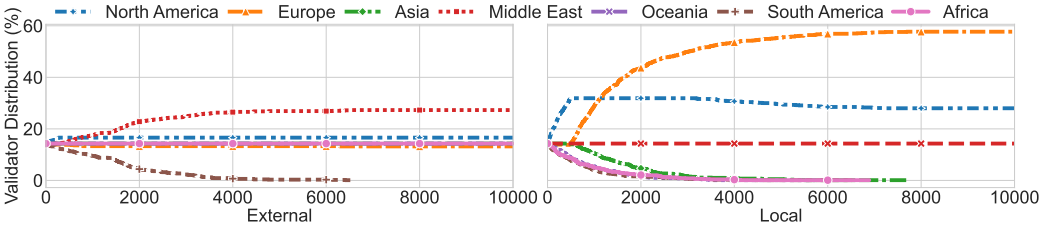


Fig. 13. *Baseline configuration (homogeneous validators and information sources).* Evolution of validator distribution aggregated by macro-regions under Local and External block-building paradigms. Early termination of a line indicates that no validators remain located within the corresponding macro-region.

G Joint Heterogeneity: Validator Convergence Locus

Figure 14 illustrates how validators redistribute across macro-regions over time in the joint-heterogeneity setting of Section 4.5, combining latency-aligned and latency-misaligned information-source placements with the empirically observed validator distribution, which is initially concentrated in Europe and North America.

Consistent with the results in Section 4.6, starting from an already concentrated validator distribution results in rapid stabilization of validator locations, with little subsequent redistribution

across regions. Consequently, only a small fraction of validators relocate under most configurations: modest migration toward North America occurs under both latency-aligned and latency-misaligned placements in the local block-building paradigm, as well as under the latency-aligned configuration in the external block-building paradigm. The existing concentration of validators in North America and Europe creates favorable propagation conditions to attesters, which continue to outweigh incentives to migrate elsewhere, even when information sources are located in other regions, under the local block-building paradigm.

A distinct pattern emerges under the external block-building paradigm when information sources are located in high-latency regions, as shown in the upper-right panel of Figure 14. In this configuration, validator mass shifts away from incumbent hubs and converges toward the supplier region, despite the initial concentration in North America and Europe. This occurs because block dissemination originates from the supplier, so proximity to other validators provides little benefit, while proximity to the supplier becomes the dominant factor shaping validator placement. As a result, validators ultimately concentrate in a single supplier region, leading to renewed geographical centralization.

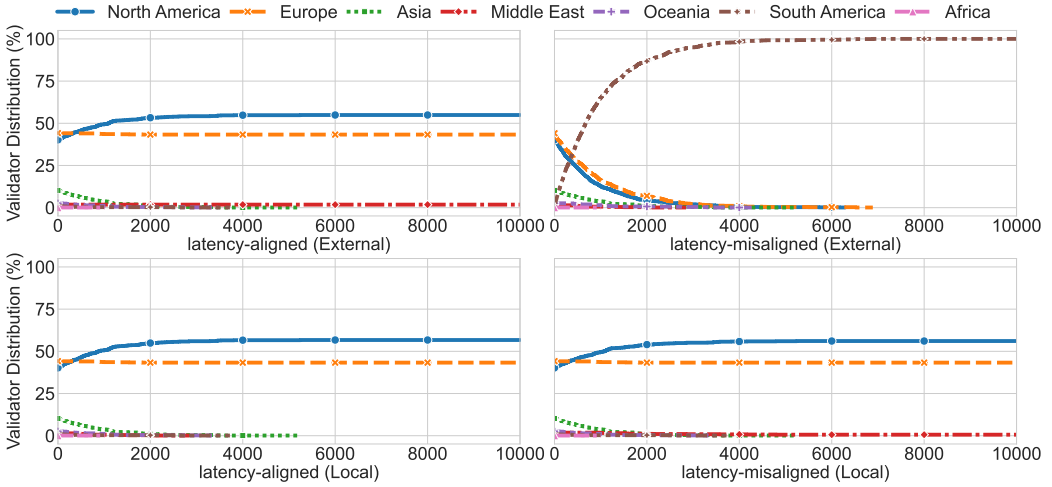


Fig. 14. *Joint heterogeneity (validators and information sources)*. Evolution of validator distribution aggregated by macro-regions under Local and External block-building paradigms for latency-aligned and latency-misaligned information-source placements with a heterogeneous validator distribution. Early termination of a line indicates that no validators remain located within the corresponding macro-region.